Korean J. Chem. Eng., 39(9), 2542-2547 (2022)
DOI: 10.1007/s11814-022-1179-z

pISSN: 0256-1115
eISSN: 1975-7220

Composites of poly(vinyl pyrrolidone) and polarized Ag nanoparticles for CO_2 separation

Beom Jun Kim* and Sang Wook Kang*,,†**

*Department of Chemistry, Sangmyung University, Seoul 03016, Korea
**Department of Chemistry and Energy Engineering, Sangmyung University, Seoul 03016, Korea
(*Received 16 November 2021 • Revised 20 March 2022 • Accepted 14 May 2022*)

Abstract−A poly(vinyl pyrrolidone) (PVP)/Ag nanoparticles (AgNPs)/7,7,8,8-Tetracyanoquinodimethane (TCNQ)/dioctyl phthalate (DOP) composite membrane using positively charged silver nanoparticles was prepared for CO_2 separation. Positively polarized silver nanoparticles were generated by TCNQ, known as an electron acceptor for CO_2 carrier. In the separation of CO_2 and N_2, the composite membrane consisting of PVP/AgNPs/TCNQ/DOP showed that only polar CO_2 could be selectively separated by a reversible reaction with the positively polarized silver nanoparticles. Furthermore, the addition of DOP as a plasticizer enhanced gas permeance through the glassy PVP, and the CO_2/N_2 selectivity performance reached 103.8. The PVP/AgNPs/TCNQ/DOP composite membranes were characterized by FT-IR spectroscopy, X-ray photoelectron spectroscopy, thermogravimetric analysis, and scanning electron microscopy.

Keywords: Ag Nanoparticle, DOP, TCNQ, Olefin, Facilitated Transport

INTRODUCTION

Global warming, mainly induced by greenhouse gases, is a serious problem that causes environmental issues such as climate change, a rise in the average sea level, and ozone depletion [1-3]. Increasing greenhouse gas emissions from many sources are accelerating global warming. In particular, the combustion of fossil fuels, which has the greatest impact on global warming, is raising the concentration of greenhouse gases in the atmosphere, even though new and renewable forms of energy are taking their place [4]. Above all, CO_2 is the major contributor to greenhouse gases, accounting for about 80% of their total content in the atmosphere and having an enormous effect on global warming [5].

For these reasons, it is of great importance to reduce greenhouse gases in the atmosphere, particularly CO_2, through carbon capture and storage (CCS) techniques to sustain human life and reverse global warming. Many studies have found that when CCS is applied to post-combustion CO_2 reduction, more than 90% of the CO_2 can be reduced, and research is being conducted in various fields [6,7]. Zhao et al. [8] reported porous activated carbon for CO_2 capture from sugarcane bagasse owing to concerns regarding solid CO_2 cost. In this study, porous activated carbon was activated by using activating agents such as air, NaOH, H_3PO_4, and CO_2, showing a high CO_2 adsorption performance of 4.28 mmol CO_2/g at 25 °C and 1 bar, particularly NaOH-activated carbon (CAC-S). Furthermore, CCS technology using an electric field was recently studied. Wang et al. [9] reported the use of a penta-graphene (PG) nanosheet to adsorb and separate CO_2 by applying an electric field. They argued that electrically activated PG nanosheets can chemically interact with CO_2, but not H_2 or CH_4, owing to the strong binding energy of PG nanosheets. This study implied that CO_2 capture and separation can be controlled by turning on and off the electric field.

Among numerous CO_2 permeation technologies, including adsorption, absorption, cryogenic distillation, and chemical looping, technology that applies a separation membrane using a thin selective film to allow the permeation of a specific gas is attracting attention for its advantages [10-13]. Membrane technology for CO_2 separation has the advantages of energy savings, low cost, and easy operation, which can lead to its commercial use. Gas separation using a separation membrane is determined by the relative velocity difference of each gas passing through the separation membrane, which follows the solution-diffusion process and Fickian law [14]. Membranes can be classified according to their many structural differences. In the case of CO_2 separation membranes, dense membranes composed of substances that selectively react with CO_2 are widely used [15]. CO_2 has properties that are physically and chemically different from gases such as N_2 and CH_4 and can be separated by selective reactions.

In recent years, metal organic frameworks (MOFs) in membranes have attracted attention as a promising method for CO_2 adsorption with high porosity, wide reaction range, and pore size control [16-18]. Jin et al. [19] introduced a novel metal organic framework, MOF-81, which was incorporated in a polyester-block-amide (PEBA) polymer formed on a porous substrate via a spinning-coating method. MOF-81 has a fast and selective transport channel for CO_2 over N_2 because of its smaller kinetic diameter. The MOF-801/PEBA mixed matrix membrane (MMM) showed high performance, showing 22.4 GPU of CO_2 permeance and a CO_2/N_2 selectivity of 66. Furthermore, research on covalent organic frameworks (COF) is underway [20,21]. COF is composed of light elements and is receiving growing attention owing to its unique pore size, structural diversity, and functionalized wall, leading to CO_2 separation performance. Zhang et al. [22] reported a COF-5 nanosheet by a sonochemical method and fabricated MMM dis-

†To whom correspondence should be addressed.
E-mail: swkang@smu.ac.kr

persed in PEBAX-1657 polymer. The COF-5/PEBAX-1657 MMM showed a selectivity of 49.3 and 493 Barrer for CO_2/N_2 separation due to the expansion effect.

To overcome these shortcomings and improve membrane performance, further research is being carried out [23-26]. Our lab has been studying CO_2/N_2 separation using various nanoparticles in ionic liquids [27-30]. In a previous study, a liquid-state membrane containing CdO nanoparticles was prepared [28]. For the 1-butyl-3-methyl imidazolium tetrafluoroborate/CdO/1-aminopyridinium iodide membrane, the CO_2 permeance was 22.6 GPU and its selectivity was 64.6. Furthermore, to compensate for the shortcomings of the liquid state membrane, since its performance deteriorates as it soaks the polymer over time, a poly(ethylene oxide) (PEO) polymer membrane was prepared to which ZnO nanoparticles and ionic liquid were added for CO_2/N_2 separation [29]. The PEO/1-butyl-3-methyl imidazolium tetrafluoroborate ($BMIM^+BF4^-$)/ZnO nanocomposite membrane showed a CO_2 permeance of 35.7 GPU and a selectivity of 29.7. These results indicate that the oxide of metal nanoparticles interacts well with CO_2, and nanoparticles function as a barrier to N_2.

Herein, we introduce a new concept to CO_2 separation research using partially positively polarized silver nanoparticles. We fabricated a PVP nanocomposite polymer membrane capable of separating CO_2 through facilitated transport, which is one of the prospective technologies for separation membranes because of its ability to increase both selectivity and permeability by way of a carrier that only reacts with a specific substance. Silver nanoparticles partially polarized by the electron acceptor are used as carriers and will interact only with polar CO_2 to selectively allow CO_2 to permeate in CO_2/N_2 gas mixtures [31]. In addition, to overcome the limitations of PVP, which has very low gas permeability owing to its glassy property, DOP was added to increase the flexibility of the polymer. Consequently, it was expected that polar CO_2 would pass through the plasticized polymer and be separated due to the presence of silver nanoparticles.

MATERIALS AND METHODS

1. Materials

Poly(vinyl pyrrolidone) (PVP, M_w 360,000), silver tetrafluoroborate ($AgBF_4$, 98.0%), and 7,7,8,8-tetracyanoquinodimethane (TCNQ, 98.0%) were purchased from Tokyo Chemical Industry Co. Dioctyl phthalate (DOP, 99.5%) was purchased from Aldrich Chemical Co. Ethyl alcohol was purchased from Samchun Chemicals. All chemicals were used as received.

2. Membrane Preparation

PVP/$AgBF_4$/TCNQ/DOP composite membranes were prepared by adding $AgBF_4$ and TCNQ to a 3 wt% PVP solution in 94.5% ethanol. The solution was stirred at 80 °C for 10 days until a brownish yellow color was observed, indicating that silver nanoparticles were properly formed. Then, DOP was added as a plasticizer to the mixed solution. The molar ratio of PVP/$AgBF_4$/TNCQ was 1 : 1 : 0.01, and the weight ratio of DOP to PVP was fixed at 0.03. To reach an appropriate concentration and viscosity, the solution was heated at 130 °C to evaporate solvent. For the fabrication of the separative membrane, the concentrated solution was coated on a macroporous polysulfone support (Toray Chemical Korea Inc.) using an RK Control Coater (Model K202, Control Coater RK Print-Coat Instruments Ltd., UK). The coated membrane was dried at room temperature for 2 h and used immediately to measure the gas permeation performance.

3. Characterization

Scanning electron microscopy (SEM) images were collected using a JEOL JSM-5600LV. The weight loss of the composite was measured using thermogravimetric analysis (TGA, TGA Q50, TA Instruments) under N_2 flow. The IR data were obtained using a VERTEX 70 FT-IR spectrometer; 16 scans were signal-averaged with a resolution of 8 cm^{-1}. The XPS data were acquired using a PHI 5000 Versa Probe (Ulvac-PHI, Japan).

4. Gas Separation Experiments

All tests for gas permeation were performed by measuring the permeance of CO_2 and N_2 single gases with a bubble meter with the pressure fixed at 2 bar. The unit of gas permeance is GPU (1 GPU= 1×10^{-6} cm^3 (STP)/(cm^2 s cmHg)).

RESULTS AND DISCUSSION

1. Gas Separation

The performance of the membrane into which the polarized silver nanoparticles were introduced was measured by the permeation of carbon dioxide and nitrogen. All measurements were carried out at room temperature. Table 1 shows selectivity and CO_2 permeance of neat PVP, PVP/AgNPs/TCNQ and PVP/AgNPs/TCNQ/DOP composite membrane. These membranes show a selectivity of 103 and a permeance of 1.03 GPU for CO_2 and no measurable permeance for N_2, which was calculated as 0.01 GPU for selectivity. This low permeability can be explained by the glassy nature of PVP. However, gas transport was accelerated by the increased free volume in the plasticized regions by DOP, even though the amount of added DOP was small. DOP was added as a plasticizer to improve the low permeability of the PVP-based membrane. As shown in Table 1, permeance of neat PVP and PVP/AgNPs/TCNQ was not measurable and as DOP was incorporated, the permeance for CO_2 increased to 1.0 GPU. The permeance of N_2 and CO_2 can be explained as follows: polar CO_2 gases with high quadrupole moment values can be selectively transported by way of the silver nanoparticles positively polarized by TNCQ as a carrier, while non-polar N_2 molecules cannot permeate. In addition, CO_2 permeability is ob-

Table 1. Selectivity and CO_2 permeance of PVP/AgNPs/TCNQ/DOP composite membrane

	Selectivity (CO_2/N_2)	CO_2 permeance (GPU)
Neat PVP [32]	Not measurable	Not measurable
PVP/AgNPs/TCNQ	Not measurable	Not measurable
PVP/AgNPs/TCNQ/DOP	103	1.0

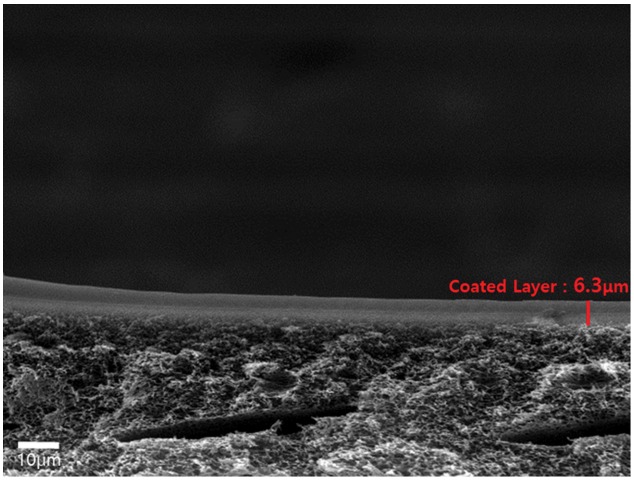

Fig. 1. Cross-sectional SEM image of PVP/AgNPs/TCNQ/DOP composite membrane on polysulfone microporous support.

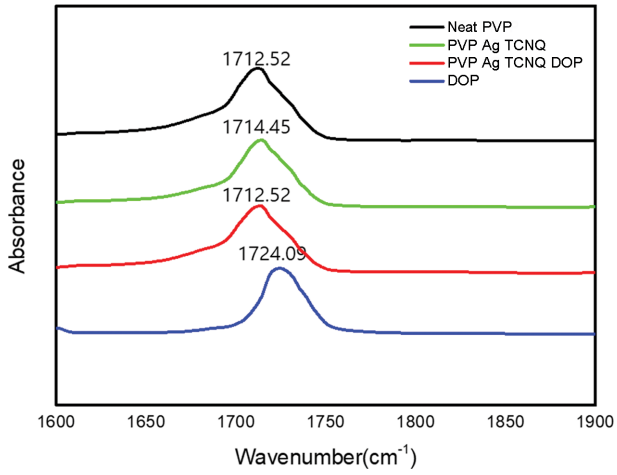

Fig. 2. FT-IR spectra of neat PVP, PVP/Ag nanoparticle/TCNQ, PVP/Ag nanoparticle/TCNQ/DOP and DOP.

served because the interaction between CO_2 and silver nanoparticles is a sufficiently weak interaction under pressure.

2. Scanning Electron Microscopy (SEM) Images of Composite Membranes

SEM images were obtained to confirm the thickness of the composite membrane coated on the polysulfone microporous membrane. As shown in Fig. 1, the polysulfone microporous membrane has a sponge-like structure capable of effectively allowing the permeation of gases such as CO_2 and N_2, and the composite membrane coated layer is observed to be 6.3 μm thick. In addition, considering that the thickness of the selective layer is uniform, the solution was evenly dispersed onto the support.

3. FT-IR Spectroscopy

FT-IR spectroscopy was used to investigate the interaction between silver nanoparticles, DOP, and the polymer through the carbonyl group peak. First, as shown in Fig. 2, it was confirmed that the carbonyl peak of neat PVP occurs at 1,712 cm^{-1}. When silver nanoparticles with TCNQ were added to neat PVP, the peak shifted slightly to 1,714 cm^{-1}. This result means that, as silver nanoparticles were incorporated into the brittle PVP polymer for strong dipole attraction between the chains, the distance between the chains in the polymer increased and the bond strength of the carbonyl group recovered. On the other hand, when DOP was added, the carbonyl peak slightly shifted to the left, indicating that the strength of the carbonyl bond was weakened. This result implies that the interaction between the carbonyl group of PVP and AgNPs becomes stronger as the polymer chain becomes more flexible due to the plasticizing effect of DOP.

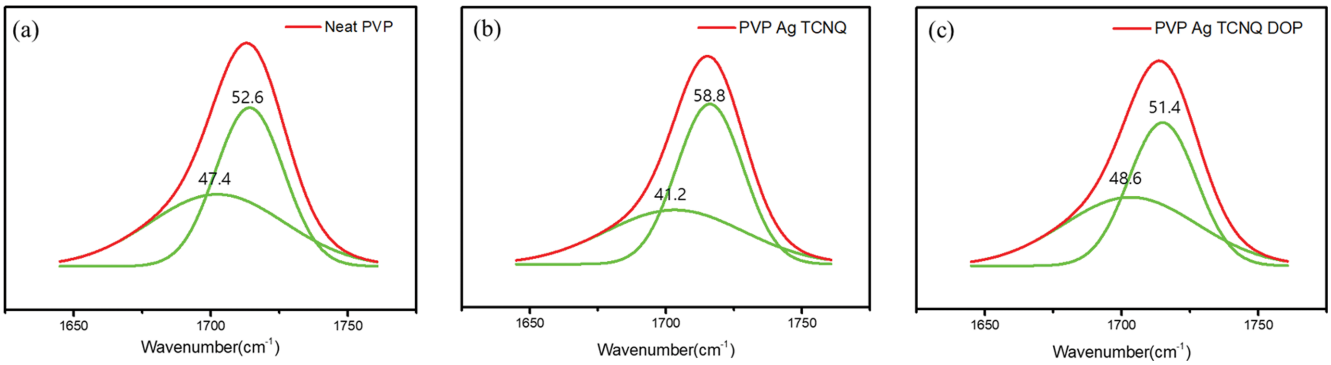

Fig. 3. Deconvolution of the carbonyl peak of FT-IR spectra: (a) neat PVP, (b) PVP/Ag nanoparticle/TCNQ, and (c) PVP/Ag nanoparticle/TCNQ/DOP composite membranes.

Table 2. Deconvoluted % data of (a) neat PVP, (b) PVP/Ag nanoparticle/TCNQ, and (c) PVP/Ag nanoparticle/TCNQ/DOP composite membranes

	1,702.3-1,703.2 cm^{-1}	1,714.2-1,716.1 cm^{-1}
Neat PVP	47.7%	52.6%
PVP/AgNPs/TCNQ	41.2%	58.8%
PVP/AgNPs/TCNQ/DOP	48.6%	51.4%

Table 3. Binding energy of silver atoms with TCNQ in composite membrane

	Ag $d_{5/2}$	Ag $d_{3/2}$
PVP/AgNPs/TCNQ/DOP	368.56	374.56
Neat AgNPs[31]	368.26	374.26

Fig. 3 and Table 2 show deconvolution data for Fig. 2. As AgNPs were added, the carbonyl peak shifted to the right, and as DOP was added, it can be confirmed that the carbonyl peaks shifted to the left. In the spectrum for the composite film to which DOP was added, a peak for DOP was not observed since its content was small.

4. X-ray Photoelectron Spectroscopy (XPS)

The electron density on the surface of the Ag NPs positively polarized by TCNQ was determined by measuring the binding energy of Ag NPs through X-ray photoelectron spectroscopy. When TCNQ is attached to the AgNP surface, the interfacial dipole is induced to shift the local vacuum energy level. Therefore, the positive transfer of vacuum energy of AgNPs is expected and, as a result, the work function increases [31]. In this study, the binding energy of Ag NPs with both TCNQ and DOP was 368.56 eV for Ag $3d_{5/2}$ and 374.56 eV for Ag $3d_{3/2}$. Compared with the previous study [31], as shown in Table 3 and Fig. 4, it is confirmed that the binding energy when TCNQ is attached to the surface of AgNPs is higher than that of neat AgNPs, at 368.26 eV and 374.26 eV for Ag $3d_{5/2}$ and Ag $3d_{3/2}$, respectively. These values indicate that TCNQ, which acts as an electron acceptor, adheres to the surface of the AgNPs and successfully generates a positive charge on the surface of the AgNPs. The positively charged AgNPs as a carrier can interact selectively with CO_2, which is more polar than N_2, thereby effectively transporting CO_2.

5. Thermogravimetric Analysis (TGA)

Neat PVP, PVP/AgNPs/TCNQ, and PVP/AgNPs/TCNQ/DOP were measured by TGA to investigate their thermal stability. Fig. 5 shows the weight loss from room temperature to 800 °C. In all measurements, the weight loss at 18-80 °C is attributed to decomposition of oligomers and low molecular weight polymers. The weight loss at 320-400 °C is due to the decomposition of PVP. The remaining weight loss at 150-300 °C is generated by an increase in the free volume as the silver nanoparticles are incorporated into the polymer chains, and thus the intermolecular attraction between the polymer chains decreases. This poor stability can be attributed to the fact that AgNPs are well dispersed in various positions and crosslinking does not occur. In the graph for PVP/AgNPs/TCNQ/DOP, a faster weight loss is observed than for those without DOP, which is attributable to the increased free volume due to the plasticization effect of DOP. These plasticizing effects are expected to accelerate gas transport through the glassy membrane.

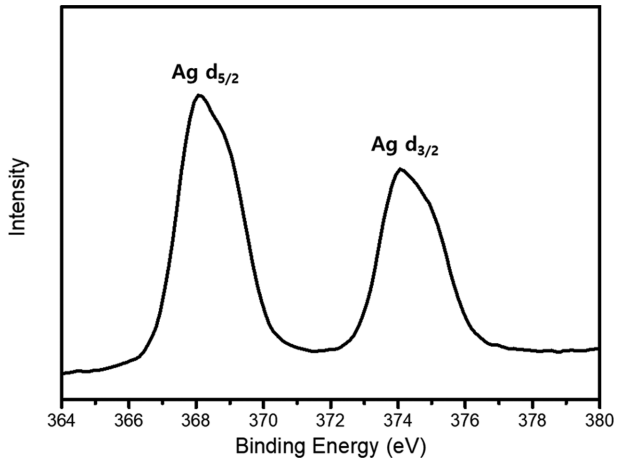

Fig. 4. Binding energy of silver atoms in PVP/AgNPs/TCNQ/DOP composite membranes.

CONCLUSION

We separated CO_2 from a CO_2/N_2 gas mixture with a facilitated transport membrane using silver nanoparticles. The composite films were characterized by IR, TGA, XPS, and SEM. The separa-

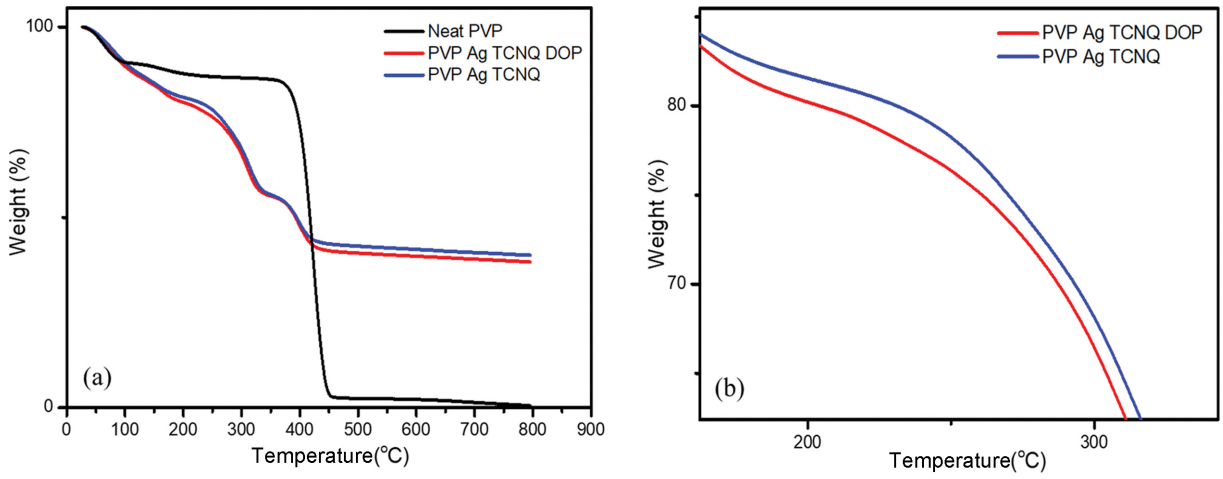

Fig. 5. TGA data of (a) neat PVP, PVP/Ag nanoparticle/TCNQ, and PVP/Ag nanoparticle/TCNQ/DOP composite membranes and (b) magnification of (a).

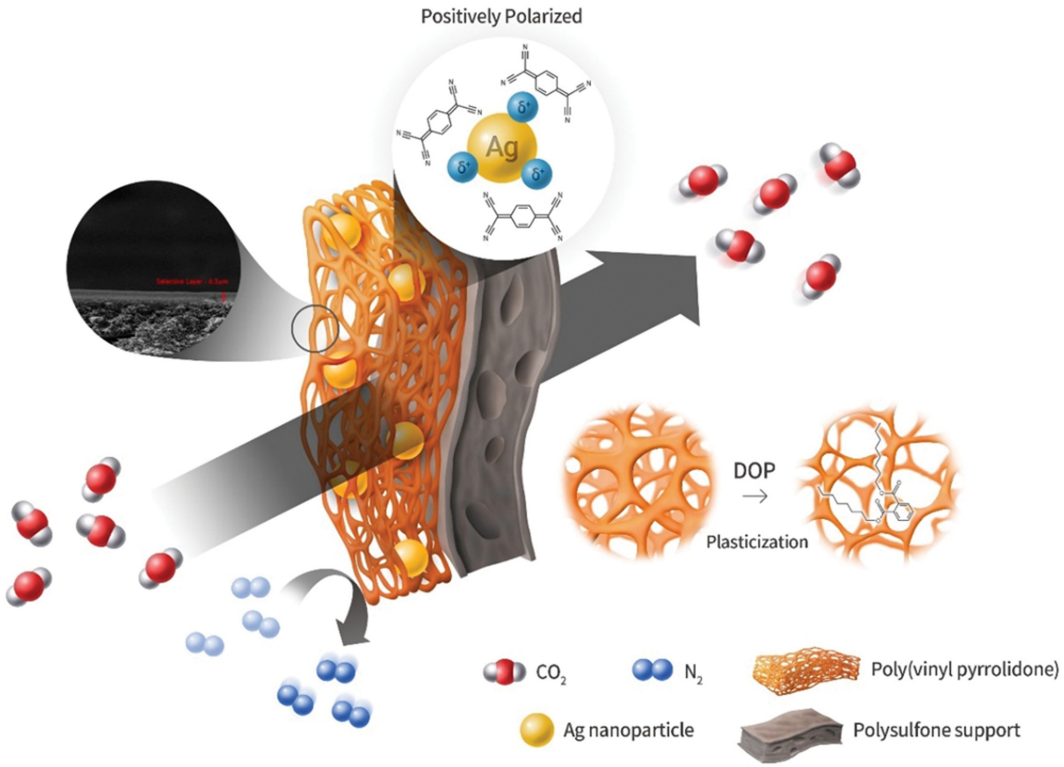

Scheme 1. CO_2 separation process in PVP/AgNPs/TCNQ/DOP composite membranes.

tion performance completely blocked the permeation of N_2 molecules and showed a selectivity of 103.8 for CO_2, as shown in Scheme 1. The blocking of N_2 transport was due to the glassy characteristics of PVP, and the permeation of CO_2 can be explained by facilitated transport, promoted by positively polarized silver nanoparticles as carriers of polar CO_2. Silver nanoparticles were positively polarized by TCNQ, which increased the binding energy compared to that of the neat silver nanoparticles. It was confirmed that the polarized silver nanoparticles could interact reversibly with CO_2 molecules. In addition, DOP was used as a plasticizer, and the resulting abundant free volume facilitated gas transport. This is the first study using polarized silver nanoparticles to show high selectivity for facilitated CO_2 transport.

ACKNOWLEDGEMENTS

This work was supported by a 2020 Sangmyung University research fund.

REFERENCES

1. X. Li, X. Lv, S. Ding, L. Huang and Z. Wei, *Int. J. Greenh. Gas Control.*, **117**, 103658 (2022).
2. T. R. Anderson, E. Hawkins and P. D. Jones, *Endeavour*, **40**(3), 178 (2016).
3. A. Dai, *Wiley Interdiscip. Rev. Clim. Change*, **2**(1), 45 (2011).
4. F. Johnsson, J. Kjärstad and J. Rootzén, *Clim. Policy*, **19**(2), 258 (2019).
5. A. Ç Köne and T. Büke, *Renew. Sustain. Energy Rev.*, **14**(9), 2906 (2010).
6. L. Selma, O. Seigo, S. Dohle and M. Siegrist, *Renew. Sustain. Energy Rev.*, **38**, 848 (2014).
7. M. Bui, C. S. Adjiman, A. Bardow, E. J. Anthony, A. Boston, S. Brown, P. S. Fennell, S. Fuss, A. Galindo and L. A. Hackett, *Energy Environ. Sci.*, **11**(5), 1062 (2018).
8. Y. Guo, C. Tan, J. Sun, W. Li, J. Zhang and C. Zhao, *Chem. Eng. J.*, **381**, 122736 (2020).
9. M. Wang, Z. Zhang, Y. Gong, S. Zhou, J. Wang, Z. Wang, S. Wei, W. Guo and X. Lu, *Appl. Surf. Sci.*, **502**, 144067 (2020).
10. A. Brunetti, F. Scura, G. Barbieri and E. Drioli, *J. Membr. Sci.*, **359**(1-2), 115 (2010).
11. W. Yave, A. Car, S. S. Funari, S. P. Nunes and K. Peinemann, *Macromolecules*, **43**(1), 326 (2010).
12. S. Hanioka, T. Maruyama, T. Sotani, M. Teramoto, H. Matsuyama, K. Nakashima, M. Hanaki, F. Kubota and M. Goto, *J. Membr. Sci.*, **314**(1-2), 1 (2008).
13. A. Yamasaki, *J. Chem. Eng. Japan*, **36**(4), 361 (2003).
14. W. Koros, G. Fleming, S. Jordan, T. Kim and H. Hoehn, *Progress Polym. Sci.*, **13**(4), 339 (1988).
15. J. Li and B. Chen, *Sep. Purif. Technol.*, **41**(2), 109 (2005).
16. S. Basu, A. Cano-Odena and I. F. Vankelecom, *Sep. Purif. Technol.*, **81**(1), 31 (2011).
17. H. Wang, L. Hou, Y. Li, C. Jiang, Y. Wang and Z. Zhu, *ACS Appl. Mater. Interfaces*, **9**(21), 17969 (2017).
18. J. Kim, S. Kim, H. Jang, G. Seo and W. Ahn, *Appl. Catal. A: Gen.*, **453**, 175 (2013).
19. J. Sun, Q. Li, G. Chen, J. Duan, G. Liu and W. Jin, *Sep. Purif. Technol.*, **217**, 229 (2019).

20. Y. Zeng, R. Zou and Y. Zhao, *Adv. Mater.*, **28**(15), 2855 (2016).
21. A. A. Olajire, *J. CO_2 Utilization*, **17**, 137 (2017).
22. K. Duan, J. Wang, Y. Zhang and J. Liu, *J. Membr. Sci.*, **572**, 588 (2019).
23. A. Ali, R. Pothu, S. H. Siyal, S. Phulpoto, M. Sajjad and K. H. Thebo, *Mater. Sci. Energy Technologies*, **2**(1), 83 (2019).
24. M. Vinoba, M. Bhagiyalakshmi, Y. Alqaheem, A. A. Alomair, A. Pérez and M. S. Rana, *Sep. Purif. Technol.*, **188**, 431 (2017).
25. N. Norahim, P. Yaisanga, K. Faungnawakij, T. Charinpanitkul and C. Klaysom, *Chem. Eng. Technol.*, **41**(2), 211 (2018).
26. X. Zhu, C. Tian, C. Do-Thanh and S. Dai, *ChemSusChem*, **10**(17), 3304 (2017).
27. Y. Choi, G. H. Hong and S. W. Kang, *J. Nanosci. Nanotechnol.*, **16**(3), 2832 (2016).
28. H. Y. Kim and S. W. Kang, *Sci. Rep.*, **9**(1), 1 (2019).
29. S. Y. Rhyu, Y. Cho and S. W. Kang, *J. Ind. Eng. Chem.*, **85**, 75 (2020).
30. H. Jeon and S. W. Kang, *Polym. Compos.*, **40**(7), 2954 (2019).
31. I. S. Chae, S. W. Kang, J. Y. Park, Y. Lee, J. H. Lee, J. Won and Y. S. Kang, *Angew. Chem.*, **123**(13), 3038 (2011).
32. J. H. Oh, Y. S. Kang and S. W. Kang, *Chem. Commun.*, **49**(86), 10181 (2013).